

Reinforcement Learning based Constrained Optimal Control: an Interpretable Reward Design [★]

Jingjie Ni ^a, Fangfei Li ^{a,b}, Xin Jin ^{b,c}, Xianlun Peng ^a, Yang Tang ^b

^a*School of Mathematics, East China University of Science and Technology, Shanghai 200237, China.*

^b*Key Laboratory of Smart Manufacturing in Energy Chemical Process, Ministry of Education, East China University of Science and Technology, Shanghai 200237, China.*

^c*Research Institute of Intelligent Complex Systems, Fudan University, Shanghai 200433, China.*

Abstract

This paper presents an interpretable reward design framework for reinforcement learning based constrained optimal control problems with state and terminal constraints. The problem is formalized within a standard partially observable Markov decision process framework. The reward function is constructed from four weighted components: a terminal constraint reward, a guidance reward, a penalty for state constraint violations, and a cost reduction incentive reward. A theoretically justified reward design is then presented, which establishes bounds on the weights of the components. This approach ensures that constraints are satisfied and objectives are optimized while mitigating numerical instability. Acknowledging the importance of prior knowledge in reward design, we sequentially solve two subproblems, using each solution to inform the reward design for the subsequent problem. Subsequently, we integrate reinforcement learning with curriculum learning, utilizing policies derived from simpler subproblems to assist in tackling more complex challenges, thereby facilitating convergence. The framework is evaluated against original and randomly weighted reward designs in a multi-agent particle environment. Experimental results demonstrate that the proposed approach significantly enhances satisfaction of terminal and state constraints and optimization of control cost.

Key words: Constrained optimal control, reinforcement learning, reward design, penalty function method, multi-agent system

1 Introduction

The free-terminal-time optimal control problem, characterized by constraints on both terminal and state conditions, is highly pertinent in practical applications, as illustrated in Table 1. In addressing this, methods such as the calculus of variations [Gregory \(2018\)](#), Pontryagin’s Maximum Principle [Paruchuri and Chatterjee \(2019\)](#), dynamic programming [Elbert et al. \(2013\)](#), and reinforcement learning (RL) [Sutton and Barto \(2018\)](#) are frequently employed. Among them, RL is highlighted owing to its model-free nature, promise to deal with the curse of dimensionality, multi-agent collaboration capability without explicit policy communication, and efficient real-time computation [Bertsekas \(2019\)](#). Despite RL’s success in complex decision-making, its application to state and terminal constraints with free terminal conditions is still developing [Gu et al. \(2024\)](#). Next, we will concisely outline RL methods for handling state and ter-

minal constraints.

In the context of state constraints, safe RL offers an effective approach to uphold safety constraints while optimizing cumulative rewards. For an extensive review of safe RL advancements, we direct readers to the comprehensive survey [Gu et al. \(2024\)](#). Among various safe RL techniques [Han et al. \(2021\)](#); [Tessler et al. \(2019\)](#), the penalty-based methods receive great attention due to their nature as first-order methods and their simplicity in implementation. Existing penalty-based methods [Sootla et al. \(2022\)](#); [Liu et al. \(2020\)](#); [Kim et al. \(2024\)](#); [Dey et al. \(2024\)](#) have demonstrated empirical effectiveness; however, they either lack rigorous theoretical justifications or may compromise the consistency between the primal and penalty-based problems. The penalized proximal policy optimization method [Zhang et al. \(2022\)](#) uniquely ensures theoretical equivalence between the original and penalty-based optimization frameworks, provided the penalty factor exceeds the maximum Lagrange multiplier. However, it does not specify the appropriate range for the penalty factor,

[★] This work is supported by the National Natural Science Foundation of China under Grants 62233005 and U2441245.

Table 1

Practical applications of free terminal time optimal control with terminal and state constraints

Problem	Terminal Constraints	State Constraints	Optimization Goals
Motion planning Li et al. (2022) ; He et al. (2023)	Given position	Collision-free	Fuel or terminal time
Formation reconfiguration Liu et al. (2022)	Relative positions	Physical limits and collision-free	Terminal time
Spacecraft rendezvous Ravaoli et al. (2022)	Rendezvous distance and safe speed	Collision-free	Fuel
Attitude control Tipaldi et al. (2022)	Given attitude and angular velocity	Physical limits of attitude	Terminal time

which is a critical issue. An excessively large penalty factor can lead to numerical instability and reduced performance [Sootla et al. \(2022\)](#); [Zhang et al. \(2022\)](#), while a factor that is not sufficiently large may fail to maintain equivalence. To address numerical instability from large penalty factors, some studies [Yan et al. \(2022\)](#) have employed curriculum learning (CL) [Bengio et al. \(2009\)](#), starting with relaxed state constraints and gradually increasing their strictness. This approach mitigates instability but does not solve the core issue of establishing explicit lower bounds for penalty weights. Within the optimization domain, proposals for explicit lower bounds on penalty weights in inequality-constrained contexts [Moradian and Kia \(2021\)](#) have been put forth. However, it presumes the differentiability and convexity of the objective function and prior knowledge that is challenging to obtain in model-free settings. In summary, identifying a computationally feasible lower bound for the penalty factor remains a significant challenge.

In addressing terminal constraints, researchers often utilize reward shaping [Li et al. \(2022\)](#); [Safaoui et al. \(2024\)](#); [He et al. \(2023\)](#); [Liu et al. \(2022\)](#); [Ravaoli et al. \(2022\)](#); [Tipaldi et al. \(2022\)](#). Typically, a positive reward is awarded to the agent for successfully meeting terminal constraints. However, this reward is sparse, failing to effectively incentivize agents to transition towards terminal states before reaching them. To facilitate effective exploration, researchers introduce guidance rewards (dense rewards) to encourage agents to approach terminal states. For example, in terms of motion planning [Li et al. \(2022\)](#); [He et al. \(2023\)](#); [Safaoui et al. \(2024\)](#), the closer an agent gets to the target, the higher the reward it receives. Nevertheless, the existing research has not yet identified a precise method for calibrating the magnitude of these two rewards. Similar to the penalty factor, a low reward for terminal constraints may lead agents to neglect these constraints, while an excessively high reward could risk numerical instability and cause agents to prioritize these rewards over other objectives. A minimal guidance reward may be eclipsed by other rewards, rendering the learning of terminal constraints and other objectives with equal priority inefficient [Huang et al. \(2022\)](#). Conversely, an excessively high guidance reward might mislead agents, as its maximization may not be equated to terminal state achievement [Ng et al. \(1999\)](#); [Booth et al. \(2023\)](#).

In summary, addressing state and terminal constraints individually poses challenges in setting the penalty factor, guidance rewards, and positive rewards for terminal constraints. We frame these challenges within the broader context of reward configuration issues. The lack

of a standardized design approach leads to several concerns [Hayes et al. \(2022\)](#); [Booth et al. \(2023\)](#): 1. Inefficient policy learning: As previously discussed, misaligned reward weightings can fail to effectively convey optimization goals and constraints to agents, resulting in suboptimal policies despite extensive training. 2. Costly reward calibration: The lack of theoretical guidance necessitates a trial-and-error approach for reward tuning and policy validation by engineers, which is intellectually demanding. 3. Lack of interpretability: Even when effective reward designs are identified for specific problems, the rationale behind the effectiveness of certain configurations over others remains unclear. This situation underscores an urgent need for our research to develop a reward design methodology for constrained optimal control scenarios.

Taken together, this paper tackles the free-terminal-time optimal control problem with terminal constraints and state constraints, by introducing a theoretically sound and practically viable reward design approach. Our contributions are threefold:

- (1) Building on [Zhang et al. \(2022\)](#); [He et al. \(2023\)](#), we explicitly define the weight ranges for each reward component, including the lower bound for the penalty factor. We theoretically demonstrate that the optimal policy derived from our reward design is indeed the optimal policy for the original constrained control problem.
- (2) Compared to [Zhang et al. \(2022\)](#); [Moradian and Kia \(2021\)](#), the reward parameters in our approach can be readily obtained within the RL framework. Specifically, the necessary reward parameters are derived by solving a series of subproblems, with each solution informing the design of rewards for the subsequent problem. Subsequently, curriculum learning (CL) is employed to apply policies from simpler subproblems to aid in solving more complex ones, thereby facilitating convergence.
- (3) We tested our reward design framework in an open-source multi-agent particle environment [Lowe et al. \(2017\)](#); [Hu et al. \(2024\)](#). Compared to the original reward settings [Lowe et al. \(2017\)](#); [Hu et al. \(2024\)](#) and those that did not effectively apply our theorems, ours achieved higher rates of state and terminal constraint satisfaction and demonstrated superior performance across optimization metrics.

The structure of this paper is as follows: Section 2 introduces the Multi-Agent RL approach and formulates the constrained optimal control problem within the Multi-Agent RL framework. Section 3 details a theoretically grounded reward design. Section 4 offers practical guide-

lines for reward design. Section 5 provides empirical evidence supporting our proposed method. Finally, Section 6 is the conclusion.

Notations : We use the following notations throughout this paper. \mathbb{R}^+ , \mathbb{R} , \mathbb{R}^m denote the sets of non-negative real numbers, real numbers, and m -dimensional vectors, respectively. $\mathbb{E}[\cdot]$ denotes the expected value operator. For $x \in \mathbb{R}^m$, the notation $\|x\|_2$ signifies the 2-norm of x .

2 Preliminary and Problem Formulation

This section introduces the Multi-Agent RL approach and formulates the constrained optimal control problem within the Multi-Agent RL framework.

2.1 Preliminary

We present a Multi-Agent RL approach within a Partially Observable Markov Decision Process (POMDP) framework, formalized as $\langle n, \mathcal{S}, \mathcal{O}, \mathcal{A}, \mathcal{P}, \mathcal{R}, \gamma \rangle$. Here, n denotes the number of agents, and $\mathcal{S} = \{s^t, t \in \mathbb{Z}^+\}$ denotes the state space. The local observation for agent i at time t is denoted by $o_i^t = \mathcal{O}(s^t, i)$. The shared action space is $\mathcal{A} = \mathcal{A}_1 \times \mathcal{A}_2 \times \dots \times \mathcal{A}_N$, with the individual action space for agent i being $\mathcal{A}_i = \{a_i^t, t \in \mathbb{Z}^+\}$. The transition probability from state s^t to s^{t+1} given the joint action $a^t = (a_1^t, \dots, a_N^t)$ is denoted by $\mathcal{P}(s^{t+1} | s^t, a^t)$. The shared reward function is $\mathcal{R}(s^t, a^t)$, and the discount factor is γ . The policy for agent i is defined as $\pi_i : o_i^t \rightarrow a_i^t, \forall t$. We define the agents' joint policy as $\pi = \pi_1 \times \pi_2 \times \dots \times \pi_n$. In this paper, we consider a fully cooperative setting where all agents share the same reward function, aiming to maximize the expected return

$$J(s^0, \pi) = \mathbb{E}\left[\sum_{t=0}^{T_f} \gamma^t \mathcal{R}(s^t, a^t)\right], \quad (1)$$

where T_f is the terminal step. The optimal joint policy can be obtained by integrating it with the general Multi-Agent RL algorithm Yu et al. (2022).

2.2 Optimal Constrained Control Problem

We consider a free-terminal-time optimal control problem for a discrete-time system of n agents, subject to terminal and state constraints. Let $x_i(t) \in \mathbb{R}^p$ and $u_i(t) \in \mathbb{R}^q$ represent the control state and control input of agent i , respectively. Define $x(t) = [x_1(t)^\top, x_2(t)^\top, \dots, x_n(t)^\top]^\top \in \mathbb{R}^{np}$ be the joint control state and $u(t) = [u_1(t)^\top, u_2(t)^\top, \dots, u_n(t)^\top]^\top \in \mathbb{R}^{nq}$ be the joint control input. Agent i can observe the control states of its m neighbors $\bar{x}_i(t) = [x_{i1}(t)^\top, x_{i2}(t)^\top, \dots, x_{im}(t)^\top]^\top$, where $x_{ij}(t)$ is the control state of the i^{th} neighbor of agent i . Our goal is to determine a policy $\pi_i : [x_i(t)^\top, \bar{x}_i(t)^\top, t]^\top \rightarrow u_i(t)$ for each agent $i = 1, 2, \dots, n$ at any time step t that

satisfies the following conditions:

$$\min_{\pi_1, \pi_2, \dots, \pi_n} \sum_{t=1}^{t_f} c(x(t), u(t)), \quad (2a)$$

$$\text{s.t. } x(0) \in \Phi, \quad (2b)$$

$$x(t+1) = f(x(t), u(t)), \quad t = 0, \dots, t_f, \quad (2c)$$

$$x(t_f) \in F, \quad (2d)$$

$$t_f < t_{\max}, \quad (2e)$$

$$x(t) \in C, \quad t = 0, \dots, t_f, \quad (2f)$$

$$u(t) \in U, \quad t = 0, \dots, t_f. \quad (2g)$$

Our optimization objective is presented in (2a), where $c : \mathbb{R}^{np} \times \mathbb{R}^{nq} \rightarrow \mathbb{R}^+$ represents the cost function. The initial joint control state is constrained to the set $\Phi \subseteq \mathbb{R}^{np}$, defined by (2b). The discrete-time system dynamics are governed by the deterministic transition function $f : \mathbb{R}^{np} \times \mathbb{R}^{nq} \rightarrow \mathbb{R}^{np}$, as described in (2c). The terminal state must remain within the set $F \subseteq \mathbb{R}^{np}$, as indicated by the terminal constraint in (2d). The control horizon is finite, limited to t_{\max} , as specified in (2e). The state must remain within the set $C \subseteq \mathbb{R}^{np}$, as indicated by the state constraint in (2f). The control input constraint is given in (2g), where $U \subseteq \mathbb{R}^{nq}$ represents the feasible set of control inputs. The problem (2) is prevalent in practice as shown in Table 1. The cost function in (2a) can be tailored for diverse objectives Lewis et al. (2012). For minimum-time, set

$$c(x(t), u(t)) = 1, \quad (3)$$

which makes (2a) equivalent to minimizing $\sum_{t=1}^{t_f} 1 = t_f$. For minimum-fuel problems, use

$$c(x(t), u(t)) = \|u(t)\|_2. \quad (4)$$

2.3 POMDP Formulation

Now, we formalize the problem (2) within the POMDP framework. First, we define $\langle \mathcal{S}, \mathcal{O}, \mathcal{A}, \mathcal{P} \rangle$. The details of $\langle \mathcal{R}, \gamma \rangle$ will be presented in subsequent sections. The state s^t is defined as the concatenation of the joint control state and the current time step, denoted as $[x(t)^\top, t]^\top$. The local observation for agent i at time t is denoted by $o_i^t = [x_i(t)^\top, \bar{x}_i(t)^\top, t]^\top$. The action for agent i is defined as $a_i^t = u_i(t)$. The transition probability $\mathcal{P}(s^{t+1} | s^t, a^t)$ is governed by the deterministic function f , as specified in (2c).

Next, we outline our approach to incorporating constraints (2b)-(2g) within the POMDP framework. First, the initial state constraint (2b) is ensured by specifying the initial state at the start of each episode. The system dynamics (2c) can be naturally incorporated into the RL framework via the transition probability function \mathcal{P} . To handle the control input constraint (2g), we consider several scenarios. If the control input is continuous and bounded, i.e., $U = \{u(t) | |u_{ij}(t)| \leq \bar{u}_{ij}(t), i = 1, \dots, n, j = 1, \dots, q\}$,

with $|u_{ij}(t)|$ being the absolute value of the j -th element of u_i and $\bar{u}_{ij}(t)$ representing its maximum allowable value, we can use an activation function like \tanh in the output layer of the policy network to ensure compliance. For a discrete control set $U = \{u^1, u^2, \dots, u^k\}$, algorithms designed for discrete actions can be applied Yu et al. (2022). For more complex forms, techniques such as action masking may be employed Rizvi and Boyle (2025). Finally, the terminal constraint (2d), the finite-time constraint (2e), and the state constraint (2f) are guaranteed by defining an appropriate terminal step T_f and $\langle \mathcal{R}, \gamma \rangle$. Specifically, for any time step, the terminal step T_f is set to t if one of the following conditions is met: (1). The terminal constraint in (2d) is satisfied; (2). The state constraint in (2f) is violated; (3). The current time step satisfies $t = t_{\max} - 1$, indicating that the next time step will violate (2e). Next, we introduce the components $\langle \mathcal{R}, \gamma \rangle$.

3 Reward Design with Theoretical Guarantees

For problem (2), the reward typically consists of four components Ravaioli et al. (2022); He et al. (2023); Liu et al. (2022); Tipaldi et al. (2022):

$$\mathcal{R}(s^t, a^t) = \alpha \mathcal{R}^a(s^t, a^t) + \beta \mathcal{R}^g(s^t, a^t) + \lambda \mathcal{R}^p(s^t, a^t) + \mu \mathcal{R}^c(s^t, a^t). \quad (5)$$

The reward for meeting the terminal constraint is:

$$\mathcal{R}^a(s^t, a^t) = \begin{cases} 1, & \text{if (2d) is satisfied,} \\ 0, & \text{otherwise.} \end{cases} \quad (6)$$

Here, we simply use 1 or 0 as the reward for whether equation (2d) is satisfied, a method that is general without loss of specificity, given that there is a weight $\alpha > 0$ associated with $\mathcal{R}^a(s^t, a^t)$ in (5). To overcome sparse rewards, the guidance reward $\mathcal{R}^g(s^t, a^t)$ steers the agent towards the terminal state:

$$\mathcal{R}^g(s^t, a^t) = l(s^t, a^t), \quad (7)$$

where $l : \mathcal{S} \times \mathcal{A} \rightarrow \mathbb{R}$ is a guidance function, with $l(s^t, a^t)$ increasing as the state approaches the terminal state. $\beta \geq 0$ is the weight of $\mathcal{R}^g(s^t, a^t)$. $\mathcal{R}^p(s^t, a^t)$ is the penalty for state constraint violation:

$$\mathcal{R}^p(s^t, a^t) = \begin{cases} 0, & \text{if (2f) is satisfied,} \\ -1, & \text{otherwise.} \end{cases} \quad (8)$$

The constant $\lambda \geq 0$ represents the weight of the penalty, with its magnitude reflecting the importance of state constraint satisfaction. The reward function $\mathcal{R}^c(s^t, a^t)$, aimed at minimizing the cumulative cost for agents, is defined as follows:

$$\mathcal{R}^c(s^t, a^t) = c(s^t, a^t), \quad (9)$$

with $\mu \leq 0$ being the weight coefficient of $\mathcal{R}^c(s^t, a^t)$. Since the cost functions are equally weighted at each time step, in (1), we set

$$\gamma = 1. \quad (10)$$

To convey the goals of the proposed problem (2) to the agents, it is crucial to define a sensible range for the reward parameters α, β, μ , and λ . To achieve this, we first establish Assumption 1 and then introduce Theorem 1, which provides sufficient conditions to ensure the consistency of the optimal joint policy that maximizes (1) and the one for the proposed problem (2).

Assumption 1. There exists a positive constant $\rho \in \mathbb{R}^+$ such that for all state-action pairs (s^t, a^t) , the inequality $|l(s^t, a^t)| < \rho$ holds, where $l : \mathcal{S} \times \mathcal{A} \rightarrow \mathbb{R}$ is the guidance function.

Prior to presenting Theorem 1, we define

$$\tau = \max_{s^0, s^{t_f}} \mathbb{E}_{\tilde{\pi}} \left[\sum_{t=1}^{T_f} c(s^t, a^t) \middle| s^0 \text{ satisfies (2b), } s^{t_f} \text{ satisfies (2d)} \right]. \quad (11)$$

Here, the cumulative control cost upper bound τ is calculated for all potential initial states s^0 and terminal states s^{t_f} under the joint policy $\tilde{\pi}$, which guarantees constraint satisfaction. Specifically, the constraint-satisfying joint policy $\tilde{\pi}$ ensures that all agents can satisfy the constraints (2b)-(2g), irrespective of the specific optimal objective (2a).

Theorem 1. For a noiseless kinematic system (2c), if β, μ , and λ satisfy the following conditions:

$$\lambda > \alpha, \quad \beta = 0, \quad \mu > -\frac{\alpha}{\tau}, \quad (12)$$

then the optimal joint policy derived from the reward (5) coincides with the optimal joint policy of the proposed problem (2).

Proof. See Appendix A. ■

Theorem 1 outlines the reward structure for an optimal policy in problem (2), which requires the guidance reward weight β to be zero and the identification of the parameter τ . However, this setup is impractical due to the sparse reward issue caused by the lack of guidance rewards and the challenge of estimating τ without prior knowledge. To overcome these issues, we introduce a practical guide for reward design in the subsequent section.

4 Reward Design with Practical Guarantees

In this section, we present a practical method for setting the guidance reward weight $\beta = 0$ and estimating τ . Initially, we suggest addressing simpler problems to gather

prerequisite knowledge for estimating the parameter τ . Then, leveraging CL, we effectively sequence these simpler problems and skillfully utilize the policies derived from solving them to set $\beta = 0$ without affecting convergence.

4.1 Reward Parameter Acquisition Process by Solving Two Subproblems

This section describes our approach to acquiring the necessary knowledge for estimating the parameter τ . To achieve this, we need to solve two subproblems: 1) the proposed problem (2), which aims to minimize the time cost function (3), known as the *minimum-time problem*, and 2) the *minimum-time problem* without state constraints (2f). We will then discuss the necessity of solving these subproblems and the methods used to address them.

First, we concentrate on the *minimum-time problem*. Upon resolution, we obtain the constraint-satisfying joint policy $\tilde{\pi}$. Using $\tilde{\pi}$, we guide agents to explore the environment and thereby determine τ (11). We now outline the solution to the *minimum-time problem*.

The reward and discount factor pair $\langle \mathcal{R}_m, \gamma_m \rangle$ for the *minimum-time problem*, which, instead of aligning with (10) and (5), adopts a straightforward and ingenious form that facilitates the establishment of theoretical guarantees. Specifically, we set the weight μ of $\mathcal{R}^c(s^t, a^t)$ to zero, thereby simplifying equation (5) to:

$$\mathcal{R}_m(s^t, a^t) = \alpha \mathcal{R}^a(s^t, a^t) + \beta \mathcal{R}^g(s^t, a^t) + \lambda \mathcal{R}^p(s^t, a^t). \quad (13)$$

To minimize the terminal time t_f , we use a discount factor $\gamma_m < 1$ in (1), encouraging agents to satisfy the terminal constraint promptly, as the discounted cumulative reward $\sum_{t=0}^{t_f} \gamma_m^t \mathcal{R}^a(s^t, a^t)$ increases with a decreasing t_f .

For the *minimum-time problem*, establishing appropriate parameter ranges for α , β , and λ is crucial. Thus, we introduce Theorem 2, providing conditions ensuring the consistency of the optimal joint policy that maximizes the cumulative of (13) and the one for the *minimum-time problem*. First, we define

$$t_c = \min_{s^0, s^{t_f}} \mathbb{E}_{\tilde{\pi}} \left[t_f \mid s^0 \text{ satisfies (2b), } s^{t_f} \text{ satisfies (2d)} \right]. \quad (14)$$

Here, $\tilde{\pi}$ is the optimal joint policy for the *minimum-time problem* without considering the state constraint (2f).

Theorem 2. For noiseless system model (2c), if β and λ satisfy the following conditions

$$\lambda > \alpha \gamma_m^{t_c - t_{\max}}, \quad \beta < \frac{\alpha \gamma_m^{t_{\max}} (1 - \gamma_m)^2}{2\rho(1 - \gamma_m^{t_{\max}})}, \quad (15)$$

then the optimal joint policy derived from the reward design (13) aligns with the optimal joint policy for the *minimum-time problem*, specifically (2) with (3).

Proof. See Appendix B. ■

Theorem 2 establishes that the reward scheme results in an optimal joint policy $\tilde{\pi}$ for the *minimum-time problem*, enabling the estimation of τ . However, the value of t_c within this reward scheme (15) remains undetermined. To ascertain t_c , akin to τ , we must first solve for the joint policy $\tilde{\pi}$ for the *minimum-time problem* without state constraints (2f). This problem employs the same $\langle \mathcal{R}_m, \gamma_m \rangle$ framework as the *minimum-time problem*, with the sole alteration being the setting of $\lambda = 0$ to account for the absence of state constraints. The specific reward parameter configurations are outlined in Corollary 1, with the proof methodologically analogous to Theorem 2.

Corollary 1. For noiseless system model (2c), if β and λ meet the following requirements

$$\lambda = 0, \quad \beta < \frac{\alpha \gamma_m^{t_{\max}} (1 - \gamma_m)^2}{2\rho(1 - \gamma_m^{t_{\max}})}, \quad (16)$$

then the optimal joint policy derived from the reward design (13) aligns with the optimal joint policy for the *minimum-time problem* objectives without considering state constraints (2f).

Proof. Refer to Appendix B. ■

Based on Corollary 1, we can obtain the joint policy $\tilde{\pi}$ for the *minimum-time problem* without state constraints (2f). Subsequently, by directing all agents to explore the environment using $\tilde{\pi}$, we can determine t_c (14).

Based on the analysis, computing τ involves three steps: 1. Solve the *minimum-time problem* without considering state constraint (2f) using Corollary 1 to obtain parameter t_c . 2. Solve the *minimum-time problem* using Theorem 2 to obtain parameter τ . 3. Solve the proposed problem (2) using Theorem 1. The three-step process for obtaining reward parameters may seem complex. Next, we present the CL method, which minimizes the impact of the complex process on convergence speed and ensures that setting the guidance reward weight β to zero does not hinder convergence.

4.2 A Practical Guide for Reward Design using Curriculum Learning

This section outlines the integration of CL Bengio et al. (2009) with RL. CL sequences the training into progressively challenging stages, each building on the policies learned in prior stages. This method enables the agent to develop policies in less complex environments before advancing to more complex ones, thereby boosting learning efficiency. The addition of CL in the complex reward parameter acquisition process offers two advantages: 1) the application of policy reduces the impact of the complex process on convergence speed, and 2) it ensures that setting the guidance reward weight β to zero does not hinder the process. Next, we present the curriculum design and its advantages in detail.

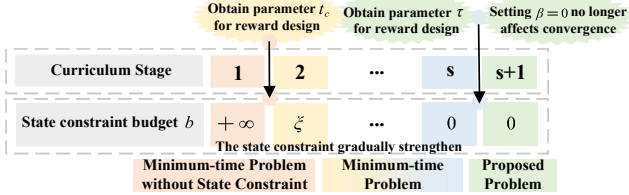


Fig. 1. Curriculum learning for reward parameter acquisition

The multi-stage curriculum is illustrated in Figure 1. Specifically, Stage 1, Stage s , and Stage $s + 1$ provide the optimal joint policies for the *minimum-time problem* without state constraints (2f), the *minimum-time problem*, and the proposed problem (2), respectively. The joint policies obtained from the first two problems provide essential information for reward design.

Solving the unconstrained *minimum-time problem* before the constrained version aligns with the CL principle of addressing simpler tasks before more complex ones. Based on this concept, we present a detailed curriculum division, as illustrated in Figure 1, for curriculum learning stages 1 to s . Without loss of generality, we define the feasible state set in (2f) as $C = \{x(t) \in \mathbb{R}^{mp} : g[x(t)] \leq 0\}$, with the state constraint budget b set to 0. In the initial stage, which addresses the *minimum-time problem* without state constraints, the constraint budget is considered as $b = +\infty$. In the subsequent stage j ($2 \leq j \leq s$), the state constraints are incrementally enforced with diminishing budget $b = \xi - \frac{(j-2)\xi}{s-2}$. Here, s is the total number of stages, and ξ is the state constraint budget for stage 2, determined based on stage 1’s adherence to state constraints. By stage s , the budget reaches zero, aligning with (2f). This method initially focuses on terminal constraints and gradually incorporates state constraints, accelerating convergence through two key strategies: 1) streamlining exploration by concentrating on transitions between initial and final states, and 2) allowing agents to learn policies in simpler scenarios with weaker constraints before addressing more complex ones. This approach avoids the inefficiency and potential convergence issues caused by excessive penalties, as discussed in Wang et al. (2023).

Moreover, at the convergence of the s^{th} curriculum stage, agents obtain a joint policy that reaches the terminal state while satisfying state constraints, eliminating the need for guidance rewards. Thus, setting the guidance reward weight $\beta = 0$ does not affect training convergence, validating the reward settings in Theorem 1.

5 Experiments

We validate our proposed reward design methodology within a multi-agent particle environment Lowe et al. (2017); Hu et al. (2024), a common RL setting, focusing on a coverage control task. As illustrated in Fig. 2, there are three agents (indicated by purple disks) and three landmarks (denoted by black disks) positioned within a two-dimensional space. The terminal constraint is satisfied when the agents com-

plete coverage of the landmarks. This is defined by the condition $\sum_{i=1}^3 \min_{k \in \{1,2,3\}} d_{ik} < 0.6$, where d_{ik} denotes the distance between agent i and landmark k . The state constraint is designed to prevent collisions among the agents, stipulating that for any two agents i and j , the distance r_{ij} between them should satisfy $r_{ij} > r = 0.3$, where r represents the safety distance. We examine two specific forms of the proposed problem (2), which differ in their optimization objectives: 1) *The minimum-time problem*; 2) *The minimum-action problem*: At each time step, an agent has the option to move “up,” “down,” “left,” “right,” or remain “stationary.” We aim to minimize the total number of actions executed by all agents. To achieve this, the cost function is defined as $c(s^t, a^t) = \sum_{i=1}^3 v_i^t$. Here, we define $v_i^t = \begin{cases} 0, & \text{if agent } i \text{ is stationary at time } t \\ 1, & \text{if agent } i \text{ moves at time } t \end{cases}$.

For both problems, we set the guidance function as $l(s^t, a^t) = 0.5 \sum_{i=1}^3 \min_{k \in \{1,2,3\}} d_{ik} + 1.35$.



Fig. 2. Coverage control task

We assess the performance using three metrics derived from results in 30 parallel simulation environments.

- (1) Terminal constraint violation rate p_ℓ^m at training step ℓ : The rate is calculated as $p_\ell^m = \frac{\sum_{k=1}^{30} z_{\ell,k}^m}{30}$, where $z_{\ell,k}^m$ is a binary indicator of terminal constraint violations in the k -th parallel environment during the episode corresponding to training step ℓ . We set $z_{\ell,k}^m = 1$ if there’s a collision or incomplete coverage; otherwise, $z_{\ell,k}^m = 0$.
- (2) State constraint violation rate p_ℓ^s at training step ℓ : This rate is denoted as $p_\ell^s = \frac{\sum_{k=1}^{30} z_{\ell,k}^s}{30}$, where $z_{\ell,k}^s$ is a binary variable indicating whether a state constraint violation occurred in the k -th parallel environment during the episode corresponding to training step ℓ . The value of $z_{\ell,k}^s$ is set to 1 if a collision occurs; otherwise, $z_{\ell,k}^s = 0$.
- (3) Optimization objective: For the *minimum-time problem*, this metric at training step ℓ is $t_\ell^f = \frac{t_{\ell,k}^f}{30}$, where $t_{\ell,k}^f$ is the terminal time in the k -th parallel environment during the episode corresponding to training step ℓ . The value of $t_{\ell,k}^f$ is set to 50 (twice the maximum time steps per episode) if any constraint is unmet; otherwise, the actual time is used. For the *minimum-action problem*, the objective for training step ℓ is $j_\ell = \frac{j_{\ell,k}}{30}$, where $j_{\ell,k}$ denotes the total actions taken in the k -th parallel environment during the episode corresponding to training step

ℓ . The value of $j_{\ell,k}$ is 75 (the product of the maximum time steps per episode and the maximum movement steps per time step) if any constraint is unmet; otherwise, the actual value is used.

Every 7500 training steps, we sample the terminal constraint violation rate p_{ℓ}^m , state constraint violation rate p_{ℓ}^s , and optimization objective t_{ℓ}^f or j_{ℓ} . Then, we calculate the average of 100 samples around each sampling point, resulting in the average terminal constraint violation rate $\overline{p_{\ell}^m}$, average state constraint violation rate $\overline{p_{\ell}^s}$, and average optimization objective $\overline{t_{\ell}^f}$ or $\overline{j_{\ell}}$. Lower values are preferable for these metrics.

The experiments are designed to address two key questions: 1). Does our proposed reward design enhance performance compared to existing frameworks? To address this, we conduct a comparative analysis of our reward scheme against established methodologies Lowe et al. (2017); Hu et al. (2024). 2). Does our reward design offer a more efficient solution relative to alternative weighting schemes? To evaluate this, we set the weight α of the reward $\mathcal{R}^{\alpha}(s^t, a^t)$ to 10 and adjust the weights of other rewards accordingly.

To ensure a fair comparison across all scenarios, we employ a consistent set of parameters as follows. Both the critic and policy networks are initialized with a single hidden layer of 64 neurons. Besides, techniques like normalization and ReLU activation are used, as in Yan et al. (2022).

5.1 Experiment for the Minimum-time Problem

We initially focus on the *minimum-time problem*, which corresponds to the proposed problem (2) with a specified optimization metric. To address question 1), we compare our reward design framework with the established one Lowe et al. (2017); Hu et al. (2024). The established framework Lowe et al. (2017); Hu et al. (2024) differs from ours in three main aspects: (1) Reward Structure: The reward settings in Lowe et al. (2017); Hu et al. (2024) differ from ours; for detailed definitions, refer to Lowe et al. (2017); Hu et al. (2024). (2) Definition of the Terminal step T_f : We set T_f to the current time step t if state constraints are violated or terminal conditions are met, whereas Lowe et al. (2017); Hu et al. (2024) does not. (3) Curriculum Learning: Our framework incorporates CL, which is not included in Lowe et al. (2017); Hu et al. (2024). In terms of our reward framework, the safe distance r , reward parameters α , λ , and β , and discount factor γ_m for each curriculum stage are summarized in Table 2. To prevent numerical instability, parameters λ and β are configured to approach their bounds according to Theorem 2 and Corollary 1. Fig. 3 illustrates the comparative analysis, demonstrating that by the final curriculum stage, our reward design (purple line) surpasses existing methods (yellow line) across all performance metrics.

With α set to 10, we evaluate the performance of reward parameters λ and β that satisfy and are near the

Table 2
Curriculum for the *minimum-time problem*

Stage	Training steps	r	α	λ	β	γ_m
1	3×10^7	0	10	/	0.035	0.99
2	2×10^7	0.25	10	12.5	0.035	0.99
3	2×10^7	0.3	10	12.5	0.035	0.99

bounds of Theorem 2, comparing it to two cases: case 1, where parameter λ or β violating Theorem 2; case 2, where parameter λ or β meeting but not nearing Theorem 2’s bound. Given these parameters are set post-curriculum stage 1, our focus is on their effects during stages 2-3. The line for case 1 is shown in the first row of the legend in Fig. 4. An insufficient penalty weight λ of 1.25 (0.1 times the value meeting and nearing the bound of Theorem 2 (VMNBT2)) incurs more state constraint breaches, as shown in the green line of Fig. 4(b). An overly large guidance reward weight β of 0.35 (10 times the VMNBT2) results in higher terminal constraint violation rates and longer terminal times due to excessive misguidance, as shown in the purple line of Fig. 4(a) and Fig. 4(c). We then assess case 2, as indicated in the last row of the legend in Fig. 4. A severe penalty weight of $\lambda = 125$ (10 times the VMNBT2) leads to increased terminal constraint violations and longer terminal times, despite ensuring state constraint compliance, as shown in the yellow line of Fig. 4(a) and Fig. 4(c). With guidance reward weight $\beta = 0$, the average metrics are similar to our method, but with higher variance, as shown in the blue line at the end of training in Fig. 4(a) and Fig. 4(c). This suggests that the absence of guidance rewards may affect robustness. Taken together, our reward scheme demonstrated superior overall performance.

5.2 Experiment for the Minimum-action Problem

Next, we focus on the *minimum-action problem*, which corresponds to the proposed problem (2) with a specified optimization metric. Solving the *minimum-action problem* requires first solving the *minimum-time problem*, as shown in Fig. 1. Specifically, the first three stages follow the curriculum outlined in Table 2 and adhere to the reward and discount factor pair $\langle \mathcal{R}_m, \gamma_m \rangle$ of the *minimum-time problem*, while the fourth stage is defined in Table 3. In our reward design framework, the parameters λ , β and μ are configured according to Theorem 1, with μ and λ positioned near their respective bounds.

Table 3
Curriculum for the *minimum-action problem*

Stage	Training steps	r	α	λ	β	μ	γ
4	4×10^7	0.3	10	10.5	0	-0.12	1

With α set to 10, we evaluate the performance of λ , μ , and β that meet and closely approach the bounds of Theorem 1, against two cases: case 1, where parameter λ , μ or β violates Theorem 1; case 2, where parameter λ , μ or β meets but does not closely approach Theorem 1’s bound. Since our reward parameters are established at the end of curriculum stage 3, we concentrate our comparison on stage 4. The analysis for case 1 is indicated in the first row of the legend in Fig. 5. An insufficient penalty weight $\lambda = 1.05$ (0.1 times the value meeting and nearing the

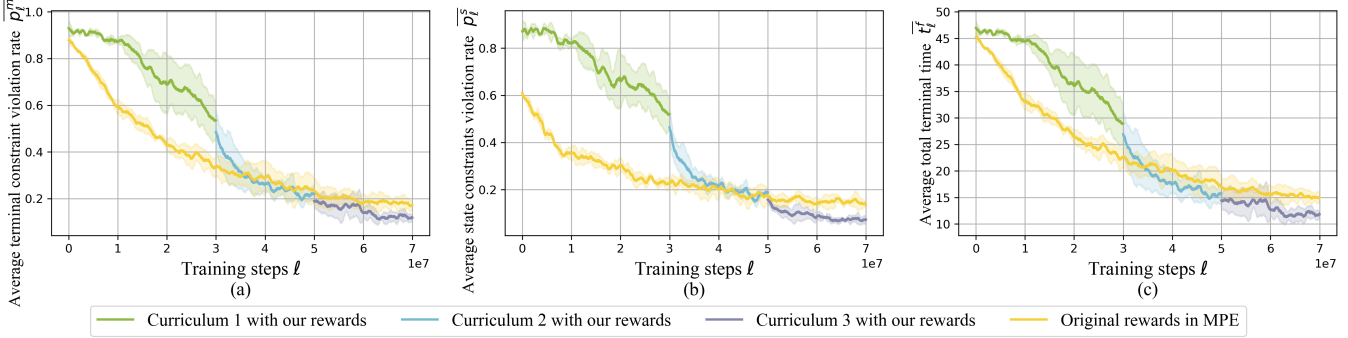


Fig. 3. Training under our reward design and the original one [Lowe et al. \(2017\)](#); [Hu et al. \(2024\)](#) for the *minimum-time problem* across 3 random seeds

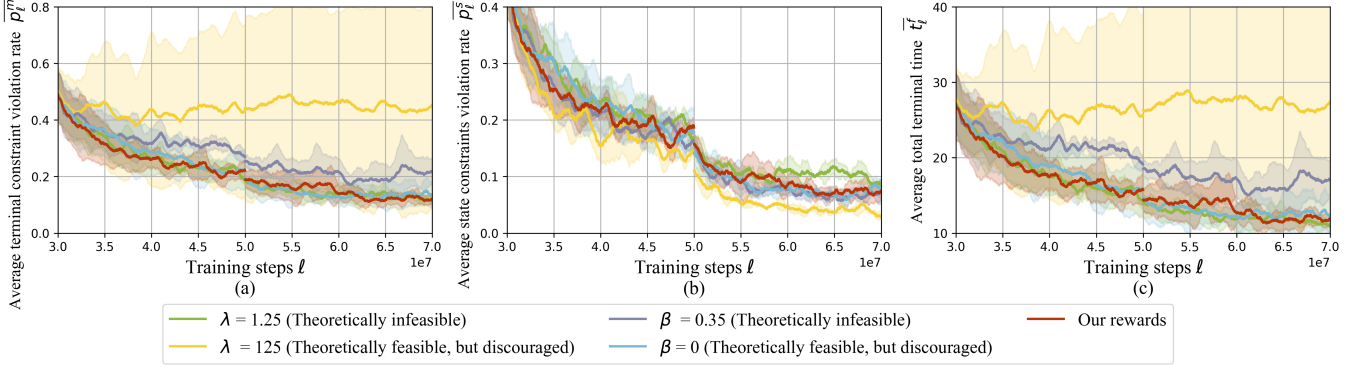


Fig. 4. Training under different reward designs for the *minimum-time problem* across 3 random seeds

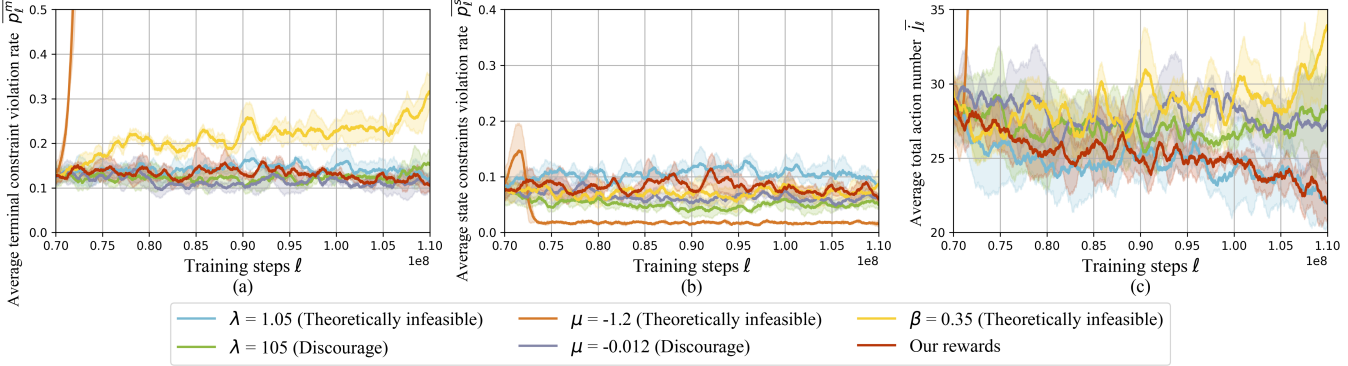


Fig. 5. Training under different reward designs for the *minimum-action problem* across 3 random seeds

bound of Theorem 1 (VMNBT1)) results in increased state constraint violations, as shown in the blue line of Fig. 5(b). The large cost function weight $\mu = -1.2$ (10 times the VMNBT1) elevates terminal constraint violation rates, as shown in the orange line of Fig. 5(a). This may be due to the movement cost overshadowing the reward for reaching the terminal state, thereby reducing its attractiveness. A large guidance reward weight $\beta = 0.35$ leads to higher terminal constraint violation rates and total action counts, as shown in the yellow line of Fig. 5(a) and Fig. 5(c). We then evaluate case 2, as indicated in the last row of the legend in Fig. 5. Setting the penalty weight $\lambda = 105$ (10 times the VMNBT1) increases total

action counts despite maintaining state constraint adherence, as shown in the green line of Fig. 5(c). This suggests that severe penalties might cause agents to focus excessively on state constraints to the detriment of other objectives. When the cost function weight $\mu = -0.012$ (0.1 times the VMNBT1) is low, the total action count does not decrease, as shown in the purple line of Fig. 5(c). In conclusion, only our reward scheme (red line) and the penalty weight $\lambda = 1.05$ (blue line) successfully minimize total actions, as shown in Fig. 5(c). Our approach outperforms the penalty weight $\lambda = 1.05$ in state constraint satisfaction, as shown in Fig. 5(b).

Remark 1. Given that the original multi-agent particle environment does not consider the minimization of total actions, we compare our reward scheme solely with alternative weight configurations.

6 Conclusion

We present a reward design framework for the RL-based multi-agent constrained optimal control problem. Initially, we provide a unified POMDP framework where the final reward is the weighted sum of four components. Subsequently, we establish bounds for the weights of these components based on theoretical proofs, ensuring that the policy maximizing the reward satisfies constraints, minimizes control cost, and avoids numerical instability. Recognizing the need for prior knowledge in the reward setting, we solve two subproblems sequentially, with each informing the reward configuration for the next. We then integrate CL with RL to apply policies from simpler subproblems to more complex ones, accelerating convergence. Experimental results demonstrate the superiority of our approach in constraint satisfaction and control cost minimization. Taken together, this paper presents a reward scheme aimed at simplifying the complex reward-tuning process for those working on RL-based optimal control problems. As the current design is tailored for deterministic systems, future research will investigate extending its applicability to systems with stochastic disturbances.

References

- Yoshua Bengio, Jérôme Louradour, Ronan Collobert, and Jason Weston. Curriculum learning. In *Proceedings of the 26th annual international conference on machine learning*, pages 41–48, 2009.
- Dimitri Bertsekas. *Reinforcement learning and optimal control*, volume 1. Athena Scientific, 2019.
- Serena Booth, W Bradley Knox, Julie Shah, Scott Niekum, Peter Stone, and Alessandro Allievi. The perils of trial-and-error reward design: misdesign through overfitting and invalid task specifications. In *Proceedings of the AAAI Conference on Artificial Intelligence*, volume 37, pages 5920–5929, 2023.
- Sumanta Dey, Pallab Dasgupta, and Soumyajit Dey. P2bpo: Permeable penalty barrier-based policy optimization for safe rl. In *Proceedings of the AAAI Conference on Artificial Intelligence*, volume 38, pages 21029–21036, 2024.
- Philipp Elbert, Soren Ebbesen, and Lino Guzzella. Implementation of dynamic programming for n -dimensional optimal control problems with final state constraints. *IEEE Transactions on Control Systems Technology*, 21(3):924–931, 2013.
- John Gregory. *Constrained optimization in the calculus of variations and optimal control theory*. Chapman and Hall/CRC, 2018.
- Shangding Gu, Long Yang, Yali Du, Guang Chen, Florian Walter, Jun Wang, and Alois Knoll. A review of safe reinforcement learning: Methods, theories and applications. *IEEE Transactions on Pattern Analysis and Machine Intelligence*, 2024.
- Minghao Han, Yuan Tian, Lixian Zhang, Jun Wang, and Wei Pan. Reinforcement learning control of constrained dynamic systems with uniformly ultimate boundedness stability guarantee. *Automatica*, 129:109689, 2021.
- Conor F Hayes, Roxana Rădulescu, Eugenio Bargiacchi, Johan Källström, Matthew Macfarlane, Mathieu Reymond, Timothy Verstraeten, Luisa M Zintgraf, Richard Dazeley, Fredrik Heintz, et al. A practical guide to multi-objective reinforcement learning and planning. *Autonomous Agents and Multi-Agent Systems*, 36(1):26, 2022.
- Zichen He, Lu Dong, Chunwei Song, and Changyin Sun. Multiagent soft actor-critic based hybrid motion planner for mobile robots. *IEEE Transactions on Neural Networks and Learning Systems*, 34(12):10980–10992, 2023.
- Yifan Hu, Junjie Fu, Guanghui Wen, Yuezu Lv, and Wei Ren. Distributed entropy-regularized multi-agent reinforcement learning with policy consensus. *Automatica*, 164:111652, 2024.
- Changxin Huang, Guangrun Wang, Zhibo Zhou, Ronghui Zhang, and Liang Lin. Reward-adaptive reinforcement learning: Dynamic policy gradient optimization for bipedal locomotion. *IEEE transactions on pattern analysis and machine intelligence*, 45(6):7686–7695, 2022.
- Yunho Kim, Hyunsik Oh, Jeonghyun Lee, Jinhyeok Choi, Gwanghyeon Ji, Moonkyu Jung, Donghoon Youm, and Jemin Hwangbo. Not only rewards but also constraints: Applications on legged robot locomotion. *IEEE Transactions on Robotics*, 40:2984–3003, 2024.
- Frank L Lewis, Draguna Vrabie, and Vassilis L Syrmos. *Optimal control*. John Wiley & Sons, 2012.
- Bin Li, Qingliang Li, Yong Zeng, Yue Rong, and Rui Zhang. 3d trajectory optimization for energy-efficient uav communication: A control design perspective. *IEEE Transactions on Wireless Communications*, 21(6):4579–4593, 2022.
- Gaoqi Liu, Bin Li, and Yuandong Ji. A modified hp-adaptive pseudospectral method for multi-uav formation reconfiguration. *ISA Transactions*, 129:217–229, 2022.
- Yongshuai Liu, Jiaxin Ding, and Xin Liu. Ipo: Interior-point policy optimization under constraints. In *Proceedings of the AAAI conference on artificial intelligence*, volume 34, pages 4940–4947, 2020.
- Ryan Lowe, Yi Wu, Aviv Tamar, Jean Harb, Pieter Abbeel, and Igor Mordatch. Multi-agent actor-critic for mixed cooperative-competitive environments. *Neural Information Processing Systems*, 2017.
- Hossein Moradian and Solmaz S Kia. Cluster-based distributed augmented lagrangian algorithm for a class of constrained convex optimization problems. *Automatica*, 129:109608, 2021.
- Andrew Y Ng, Daishi Harada, and Stuart Russell. Policy invariance under reward transformations: Theory and application to reward shaping. In *Icml*, volume 99,

pages 278–287, 1999.

Pradyumna Paruchuri and Debasish Chatterjee. Discrete time pontryagin maximum principle under state-action-frequency constraints. *IEEE Transactions on Automatic Control*, 64(10):4202–4208, 2019.

Umberto J. Ravaioli, James Cunningham, John McCarroll, Vardaan Gangal, Kyle Dunlap, and Kerianne L. Hobbs. Safe reinforcement learning benchmark environments for aerospace control systems. In *2022 IEEE Aerospace Conference (AERO)*, pages 1–20, 2022.

Danish Rizvi and David Boyle. Multi-agent reinforcement learning with action masking for uav-enabled mobile communications. *IEEE Transactions on Machine Learning in Communications and Networking*, 3:117–132, 2025. doi: 10.1109/TMLCN.2024.3521876.

Sleiman Safaoui, Abraham P. Vinod, Ankush Chakrabarty, Rien Quirynen, Nobuyuki Yoshikawa, and Stefano Di Cairano. Safe multiagent motion planning under uncertainty for drones using filtered reinforcement learning. *IEEE Transactions on Robotics*, 40:2529–2542, 2024.

Aivar Sootla, Alexander I Cowen-Rivers, Taher Jafferjee, Ziyang Wang, David H Mguni, Jun Wang, and Haitham Ammar. Sauté rl: Almost surely safe reinforcement learning using state augmentation. In *International Conference on Machine Learning*, pages 20423–20443. PMLR, 2022.

R. S. Sutton and A. G. Barto. *Reinforcement learning: An introduction*. MIT press, 2018.

Chen Tessler, Daniel J. Mankowitz, and Shie Mannor. Reward constrained policy optimization. In *International Conference on Learning Representations*, 2019.

Massimo Tipaldi, Raffaele Iervolino, and Paolo Roberto Massenio. Reinforcement learning in spacecraft control applications: Advances, prospects, and challenges. *Annual Reviews in Control*, 54:1–23, 2022.

Ziyang Wang, Yali Du, Aivar Sootla, Haitham Bou Ammar, and Jun Wang. CAMA: A new framework for safe multi-agent reinforcement learning using constraint augmentation, 2023. URL <https://openreview.net/forum?id=jK02XX9ZpJkt>.

Yuzi Yan, Xiaoxiang Li, Xinyou Qiu, Jiantao Qiu, Jian Wang, Yu Wang, and Yuan Shen. Relative distributed formation and obstacle avoidance with multi-agent reinforcement learning. In *2022 international conference on robotics and automation (ICRA)*, pages 1661–1667. IEEE, 2022.

Chao Yu, Akash Velu, Eugene Vinitsky, Jiaxuan Gao, Yu Wang, Alexandre Bayen, and Yi Wu. The surprising effectiveness of ppo in cooperative multi-agent games. *Advances in Neural Information Processing Systems*, 35:24611–24624, 2022.

Linrui Zhang, Li Shen, Long Yang, Shixiang Chen, Xueqian Wang, Bo Yuan, and Dacheng Tao. Penalized proximal policy optimization for safe reinforcement learning. In *International Joint Conference on Artificial Intelligence*, 2022.

A Proof of Theorem 1

Due to the comprehensive nature of the proof, we have organized it into 5 steps to enhance readability, with the crucial content of each step emphasized in **bold**.

Step 1. Decompose $J(s^0, \pi)$. Taking into account the noise-free system model (2c), we acquire

$$J(s^0, \pi) = \mathbb{E} \left[\sum_{t=0}^{T_f} \gamma^t \mathcal{R}(s^t, a^t) \right] = \sum_{t=0}^{T_f} \gamma^t \mathcal{R}(s^t, a^t). \quad (\text{A.1})$$

Substituting (10) into (A.1), we have

$$J(s^0, \pi) = \sum_{t=0}^{T_f} \mathcal{R}(s^t, a^t). \quad (\text{A.2})$$

Substituting (5) into (A.2), we obtain:

$$J(s^0, \pi) = \sum_{t=0}^{T_f} \left(\alpha \mathcal{R}^a(s^t, a^t) + \beta \mathcal{R}^g(s^t, a^t) + \lambda \mathcal{R}^p(s^t, a^t) + \mu \mathcal{R}^c(s^t, a^t) \right). \quad (\text{A.3})$$

Defining

$$J^a(s^0, \pi) = \sum_{t=0}^{T_f} \alpha \mathcal{R}^a(s^t, a^t). \quad (\text{A.4a})$$

$$J^g(s^0, \pi) = \sum_{t=0}^{T_f} \beta \mathcal{R}^g(s^t, a^t). \quad (\text{A.4b})$$

$$J^p(s^0, \pi) = \sum_{t=0}^{T_f} \lambda \mathcal{R}^p(s^t, a^t). \quad (\text{A.4c})$$

$$J^c(s^0, \pi) = \sum_{t=0}^{T_f} \mu \mathcal{R}^c(s^t, a^t). \quad (\text{A.4d})$$

Substituting (A.4a)-(A.4d) into (A.3), we get

$$J(s^0, \pi) = J^a(s^0, \pi) + J^g(s^0, \pi) + J^p(s^0, \pi) + J^c(s^0, \pi). \quad (\text{A.5})$$

When we substitute $\beta = 0$ into (A.4b), we derive

$$J^g(s^0, \theta) = 0. \quad (\text{A.6})$$

By substituting (A.6) into (A.5), we obtain

$$J(s^0, \pi) = J^a(s^0, \theta) + J^p(s^0, \theta) + J^c(s^0, \theta). \quad (\text{A.7})$$

Step 2. Classify policies. We categorize joint policies into four main sets $\Pi^i, i = 0, 1, 2, 3$ as shown in Table A.1.

Step 3. Analyze the components' magnitudes of

Table A.1
Policy classification

	Satisfy terminal constraint	Satisfy state constraint
Π^0	×	×
Π^1	×	✓
Π^2	✓	×
Π^3	✓	✓

$J(s^0, \pi)$ in (A.7). To analyze the magnitude of $J(s^0, \pi^i)$, where $\pi^i \in \Pi^i, i = 0, 1, 2, 3$, we first examine the individual components of $J(s^0, \pi^i)$, namely, $J^a(s^0, \pi^i)$, $J^p(s^0, \pi^i)$ and $J^c(s^0, \pi^i)$.

Firstly, based on the definition of the cost function $c : \mathbb{R}^{np} \times \mathbb{R}^{nq} \rightarrow \mathbb{R}^+$ and (9), the inequality $\mathcal{R}^c(s^t, a^t) \geq 0$ holds. Substituting this inequality and $\mu \leq 0$ into equation (A.4d), we obtain:

$$J^c(s^0, \pi_i) \leq 0. \quad (\text{A.8})$$

Next, let's consider the magnitude of $J^a(s^0, \pi_i)$. Substitute (6) into (A.4a) and consider the definition of the terminal time step T_f , we derive that

$$J^a(s^0, \pi_i) = \begin{cases} \alpha, & \text{if the terminal constraint is satisfied,} \\ 0, & \text{else.} \end{cases} \quad (\text{A.9})$$

Finally, let's examine the magnitude of $J^p(s^0, \pi_i)$. Substitute (8) into (A.4c), we obtain

$$J^p(s^0, \pi_i) = \begin{cases} -\lambda, & \text{if any state constraint is violated,} \\ 0, & \text{else.} \end{cases} \quad (\text{A.10})$$

In conclusion, we have determined the magnitudes of the individual components of $J(s^0, \pi_i)$ as shown in (A.6), (A.8), (A.9), and (A.10). Next, based on the relative magnitudes of these components, we will analyze the returns associated with each joint policy $J(s^0, \pi_i), i = 0, 1, 2, 3$.

Step 4. Compare the magnitude of returns under each policy $J(s^0, \pi_i), i = 0, 1, 2, 3$. Initially, for all $\pi^0 \in \Pi^0$, we evaluate the magnitude of $J(s^0, \pi^0)$. As per (A.7), we have

$$J(s^0, \pi^0) = J_i^c(s^0, \pi^0) + J^a(s^0, \pi^0) + J^p(s^0, \pi^0). \quad (\text{A.11})$$

According to the definition of policy set Π^0 , it is known that the agent following it has not yet satisfied the terminal constraint and state constraint. Substituting these conditions into (A.8), (A.9), and (A.10), and considering Theorem 1's conditions $\lambda > \alpha$ and $\alpha > 0$, we obtain

$$\begin{cases} J^c(s^0, \pi^0) \leq 0, \\ J^a(s^0, \pi^0) = 0, \\ J^p(s^0, \pi^0) = -\lambda < -\alpha < 0. \end{cases} \quad (\text{A.12})$$

Through substitution of equation (A.12) into equation (A.11), we conclude that

$$J(s^0, \pi^0) < 0. \quad (\text{A.13})$$

Subsequently, for all $\pi^1 \in \Pi^1$, we analyze the magnitude of $J(s^0, \pi^1)$. According to equation (A.7), we obtain

$$J(s^0, \pi^1) = J_i^c(s^0, \pi^1) + J^a(s^0, \pi^1) + J^p(s^0, \pi^1). \quad (\text{A.14})$$

According to the definition of policy Π^1 , it is known that the agent following it has satisfied the state constraint but violated the terminal constraint. Substituting these conditions into (A.8), (A.9), and (A.10), we obtain

$$\begin{cases} J^c(s^0, \pi^1) \leq 0, \\ J^a(s^0, \pi^1) = 0, \\ J^p(s^0, \pi^1) = 0. \end{cases} \quad (\text{A.15})$$

Replace (A.15) into (A.14), resulting in

$$J(s^0, \pi^1) \leq 0. \quad (\text{A.16})$$

In the following, for all $\pi^2 \in \Pi^2$, we analyze the magnitude of $J(s^0, \pi^2)$. As indicated by (A.7), we have

$$J(s^0, \pi^2) = J^c(s^0, \pi^2) + J^a(s^0, \pi^2) + J^p(s^0, \pi^2). \quad (\text{A.17})$$

By the definition of policy set Π^2 , it is established that the agent following it has satisfied terminal constraint but violated state constraints. By incorporating these conditions into (A.8), (A.9), and (A.10), we find that

$$\begin{cases} J^c(s^0, \pi^2) \leq 0, \\ J^a(s^0, \pi^2) = \alpha, \\ J^p(s^0, \pi^2) = -\lambda. \end{cases} \quad (\text{A.18})$$

By incorporating (A.18) into (A.17), we have

$$J(s^0, \pi^2) \leq \alpha - \lambda. \quad (\text{A.19})$$

Then, by substituting $\lambda > \alpha$ in (12) into (A.19), we obtain

$$J(s^0, \pi^2) < 0. \quad (\text{A.20})$$

Lastly, for all $\pi^3 \in \Pi^3$, we analyze the magnitude of $J(s^0, \pi^3)$. According to (A.7), we have

$$J(s^0, \pi^3) = J^c(s^0, \pi^3) + J^a(s^0, \pi^3) + J_m^p(s^0, \pi^3). \quad (\text{A.21})$$

According to the definition of policy set Π^3 , it is known that the agent following it has satisfied the terminal constraint and the state constraint. Incorporating these conditions into (A.9) and (A.10), we have

$$\begin{cases} J^a(s^0, \pi^3) = \alpha, \\ J_m^p(s^0, \pi^3) = 0. \end{cases} \quad (\text{A.22})$$

Substitute (A.22) into (A.21), we arrive at

$$J(s^0, \pi^3) = J^c(s^0, \pi^3) + \alpha. \quad (\text{A.23})$$

The estimation of the magnitude of $J^c(s^0, \pi^3)$ is displaced below. Based on the definition of policy $\tilde{\pi}$, it can be known that $\tilde{\pi} \in \Pi^3$. Substitute (11) into (A.4d) and take into account that $\mu < 0$, we can conclude that

$$J^c(s^0, \tilde{\pi}) \geq \mu\tau, \quad \tilde{\pi} \in \Pi^3. \quad (\text{A.24})$$

Substitute (A.24) into (A.23), we have

$$J(s^0, \tilde{\pi}) \geq \mu\tau + \alpha, \quad \tilde{\pi} \in \Pi^3. \quad (\text{A.25})$$

Substitute $\mu > -\frac{\alpha}{\tau}$ in (12) into (A.25), we find that

$$J(s^0, \tilde{\pi}) > -\alpha + \alpha = 0, \quad \tilde{\pi} \in \Pi^3. \quad (\text{A.26})$$

To sum up, according to (A.13), (A.16) and (A.20), for all $\pi^{0,1,2} \in \Pi^0 \cup \Pi^1 \cup \Pi^2$, it holds that $J(s^0, \pi^{0,1,2}) \leq 0$. According to (A.26), there exist $\tilde{\pi} \in \Pi^3$ such that $J(s^0, \tilde{\pi}) > 0$. Thus, we derive

$$J(s^0, \tilde{\pi}) > J(s^0, \pi^{0,1,2}), \quad \forall \pi^{0,1,2} \in \Pi^0 \cup \Pi^1 \cup \Pi^2. \quad (\text{A.27})$$

Step 5. Prove that the policy $\pi^{3*} \in \Pi^3$ that satisfies $J^c(s^0, \pi^{3*}) \geq J^c(s^0, \pi^3), \forall \pi^3 \in \Pi^3$ is the one with the maximum return.

According to inequality $J^c(s^0, \pi^{3*}) \geq J^c(s^0, \pi^3), \forall \pi^3 \in \Pi^3$, we can derive that

$$J^c(s^0, \pi^{3*}) \geq J^c(s^0, \tilde{\pi}). \quad (\text{A.28})$$

Substitute equation (A.28) into equation (A.23), we get

$$J(s^0, \pi^{3*}) \geq J(s^0, \tilde{\pi}). \quad (\text{A.29})$$

Insert (A.29) into (A.27), we have

$$J(s^0, \pi^{3*}) > J(s^0, \pi^{0,1,2}), \quad \forall \pi^{0,1,2} \in \Pi^0 \cup \Pi^1 \cup \Pi^2. \quad (\text{A.30})$$

Besides, in keeping with equation $J^c(s^0, \pi^{3*}) \geq$

$J^c(s^0, \pi^3), \forall \pi^3 \in \Pi^3$ and (A.23), we have

$$J(s^0, \pi^{3*}) \geq J(s^0, \pi^3), \quad \forall \pi^3 \in \Pi^3 \quad (\text{A.31})$$

Following (A.30) and (A.31), we can conclude that for all $\pi^{0,1,2,3} \in \Pi^0 \cup \Pi^1 \cup \Pi^2 \cup \Pi^3$, if $J^c(s^0, \pi^{3*}) > J^c(s^0, \pi^3), \forall \pi^3 \in \Pi^3$ then $J(s^0, \pi^{3*}) \geq J(s^0, \pi^{0,1,2,3})$. In conclusion, it can be summarized that the policy π^{3*} , which is the optimal solution to the problem (2), is the one with the maximum return.

B Proof of Theorem 2

Due to the extensive nature of the proof, for improved readability, we have divided it into 9 steps, with the key content of each step highlighted in **bold**.

Step 1. Decompose $J(s^0, \pi)$. Considering the noise-free system model (2c), we obtain

$$J(s^0, \pi) = \mathbb{E} \left[\sum_{t=0}^{T_f} \gamma_m^t \mathcal{R}_m(s^t, a^t) \right] = \sum_{t=0}^{T_f} \gamma_m^t \mathcal{R}_m(s^t, a^t). \quad (\text{B.1})$$

Substituting (13) into (B.1), we obtain:

$$J(s^0, \pi) = \sum_{t=0}^{T_f} \gamma_m^t \left(\alpha \mathcal{R}^a(s^t, a^t) + \beta \mathcal{R}^g(s^t, a^t) + \lambda \mathcal{R}^p(s^t, a^t) \right). \quad (\text{B.2})$$

Defining

$$J_m^a(s^0, \pi) = \sum_{t=0}^{T_f} \alpha \gamma_m^t \mathcal{R}^a(s^t, a^t). \quad (\text{B.3a})$$

$$J_m^g(s^0, \pi) = \sum_{t=0}^{T_f} \beta \gamma_m^t \mathcal{R}^g(s^t, a^t). \quad (\text{B.3b})$$

$$J_m^p(s^0, \pi) = \sum_{t=0}^{T_f} \lambda \gamma_m^t \mathcal{R}^p(s^t, a^t). \quad (\text{B.3c})$$

Substituting (B.3a)-(B.3c) into (B.2), we get

$$J(s^0, \pi) = J_m^a(s^0, \pi) + J_m^g(s^0, \pi) + J_m^p(s^0, \pi). \quad (\text{B.4})$$

Step 2. Calculate the upper bound of $|J_m^g(s^0, \pi)|$. Substituting (7) into (B.3b), we have

$$\begin{aligned} |J_m^g(s^0, \pi)| &= \left| \sum_{t=0}^{T_f} \gamma_m^t \beta l(s^t, a^t) \right| \quad (\text{B.5}) \\ &\leq \left| \sum_{t=0}^{T_f} \beta \gamma_m^t \right| |l(s^t, a^t)| \\ &= \left| \beta \frac{1 - \gamma_m^{T_f+1}}{1 - \gamma_m} \right| |l(s^t, a^t)|. \end{aligned}$$

Substituting the inequality $|l(s^t, a^t)| < \rho$ from Assumption 1 into (B.5), we obtain

$$|J_m^g(s^0, \pi)| < \rho\beta \frac{1 - \gamma_m^{T_f+1}}{1 - \gamma_m}. \quad (\text{B.6})$$

According to the definition of the terminal step T_f , once the current time step satisfies $t = t_{\max} - 1$, we define $T_f = t$. Thus, it follows that the inequality $T_f \leq t_{\max} - 1$ holds. Substituting this inequality into (B.6), we get

$$|J_m^g(s^0, \pi)| < \rho\beta \frac{1 - \gamma_m^{t_{\max}}}{1 - \gamma_m}. \quad (\text{B.7})$$

Taking into account $\beta < \frac{\alpha\gamma_m^{t_{\max}}(1-\gamma_m)^2}{2\rho(1-\gamma_m^{t_{\max}})}$, we can obtain the following inequality

$$|J_m^g(s^0, \theta)| < \frac{\alpha\gamma_m^{t_{\max}}(1-\gamma_m)}{2}. \quad (\text{B.8})$$

Step 3. Classify policies and explore the returns relationships. Firstly, we categorize the joint policies into 4 major sets $\Pi^i, i = 0, 1, 2, 3$, as shown in Table A.1. In the following, we reveal that for all $\pi^3 \in \Pi^3$, and for all $\pi^{0,1,2} \in \Pi^0 \cup \Pi^1 \cup \Pi^2$, it holds that $J(s^0, \pi^3) > J(s^0, \pi^{0,1,2})$.

Step 4. Prove that $J(s^0, \pi^3) > J(s^0, \pi^0)$, for all $\pi^3 \in \Pi^3$ and $\pi^0 \in \Pi^0$. First, let's consider $J(s^0, \pi^0)$. According to the definition of policy set Π^0 and rewards (6) and (8), for all $\Pi_0 \in \mathbf{\Pi 0}$, we have

$$\begin{cases} J_m^p(s^0, \pi^0) < 0, \\ J_m^a(s^0, \pi^0) = 0. \end{cases} \quad (\text{B.9})$$

Replace (B.9) into (B.4), we have

$$J(s^0, \pi^0) < J_m^g(s^0, \pi^0). \quad (\text{B.10})$$

Next, let's analyze the magnitude of $J(s^0, \pi^3)$. According to the definition of policy set Π^3 and rewards (6) and (8), for all $\pi^3 \in \Pi^3$, it leads to

$$\begin{cases} J_m^p(s^0, \pi^3) = 0, \\ J_m^a(s^0, \pi^3) > \alpha\gamma_m^{t_{\max}}. \end{cases} \quad (\text{B.11})$$

Through substitution of (B.11) into (B.4), we obtain

$$J(s^0, \pi^3) > \alpha\gamma_m^{t_{\max}} + J_m^g(s^0, \pi^3). \quad (\text{B.12})$$

According to (B.10) and (B.12), we have

$$\begin{aligned} & J(s^0, \pi^3) - J(s^0, \pi^0) \\ & > \alpha\gamma_m^{t_{\max}} + J_m^g(s^0, \pi^3) - J_m^g(s^0, \pi^0). \end{aligned} \quad (\text{B.13})$$

In accordance with (B.8), one has

$$J_m^g(s^0, \pi^3) - J_m^g(s^0, \pi^0) > -\alpha\gamma_m^{t_{\max}}(1 - \gamma_m). \quad (\text{B.14})$$

Incorporating (B.14) into (B.13), we have

$$J(s^0, \pi^3) - J(s^0, \pi^0) > \alpha\gamma_m^{t_{\max}} - \alpha\gamma_m^{t_{\max}}(1 - \gamma_m) > 0. \quad (\text{B.15})$$

Therefore, for all $\pi^3 \in \Pi^3$ and $\pi^0 \in \Pi^0$, we can conclude that $J(s^0, \pi^3) > J(s^0, \pi^0)$.

Step 5. Prove that $J(s^0, \pi^3) > J(s^0, \pi^1)$, for all $\pi^3 \in \Pi^3$ and $\pi^1 \in \Pi^1$. Considering $J(s^0, \pi^1)$, based on the definition of policy set Π^1 and rewards (6) and (8), for all $\pi^1 \in \Pi^1$, we have

$$\begin{cases} J_m^p(s^0, \pi^1) = 0, \\ J_m^a(s^0, \pi^1) = 0. \end{cases} \quad (\text{B.16})$$

Replace (B.16) into (B.4), we obtain

$$J(s^0, \pi^1) = J_m^g(s^0, \pi^1). \quad (\text{B.17})$$

In accordance with (B.17) and (B.12), it can be obtained

$$J(s^0, \pi^3) - J(s^0, \pi^1) > \alpha\gamma_m^{t_{\max}} + J_m^g(s^0, \pi^3) - J_m^g(s^0, \pi^1). \quad (\text{B.18})$$

According to equation (B.8), we have

$$J(s^0, \pi^3) - J(s^0, \pi^1) > \alpha\gamma_m^{t_{\max}} - \alpha\gamma_m^{t_{\max}}(1 - \gamma_m) > 0. \quad (\text{B.19})$$

Here, we can infer that $J(s^0, \pi^3) > J(s^0, \pi^1)$, for all $\pi^3 \in \Pi^3$ and $\pi^1 \in \Pi^1$.

Step 6. Categorize the analysis based on the final time under policy set Π^2 and Π^3 . Without loss of generality, let us fix the initial state s^0 and consider two cases based on the time required to reach the terminal state following policy sets Π^2 and Π^3 :

- Case 1. $T_{\pi_1^2} \geq T_{\pi_1^3}$, where $T_{\pi_1^2}$ denotes the time required to satisfy the terminal constraint under policy $\pi_1^2 \in \Pi^2$, and $T_{\pi_1^3}$ denotes the time required under policy $\pi_1^3 \in \Pi^3$.
- Case 2. $T_{\pi_2^2} < T_{\pi_2^3}$, where $T_{\pi_2^2}$ denotes the time required to satisfy the terminal constraint under policy $\pi_2^2 \in \Pi^2$, and $T_{\pi_2^3}$ denotes the time required under policy $\pi_2^3 \in \Pi^3$.

Below, for the above two cases, we will sequentially demonstrate that for any $\pi^2 \in \Pi^2$ and any $\pi^3 \in \Pi^3$, we have $J(s^0, \pi^2) < J(s^0, \pi^3)$.

Step 7. Prove that $J(s^0, \pi_1^3) > J(s^0, \pi_1^2)$, for all $\pi_1^3 \in \Pi^3$ and $\pi_1^2 \in \Pi^2$ with $T_{\pi_1^2} \geq T_{\pi_1^3}$. For any $\pi_1^2 \in \Pi^2$ and

any $\pi_1^3 \in \Pi^3$ satisfying $T_{\pi_1^2} \geq T_{\pi_1^3}$, we have

$$\begin{cases} J_m^a(s^0, \pi_1^2) = \alpha \gamma_m^{T_{\pi_1^2}}, \\ J_m^a(s^0, \pi_1^3) = \alpha \gamma_m^{T_{\pi_1^3}}. \end{cases} \quad (\text{B.20})$$

Since $T_{\pi_1^2} \geq T_{\pi_1^3}$, the inequality $\alpha \gamma_m^{T_{\pi_1^2}} \leq \alpha \gamma_m^{T_{\pi_1^3}}$ holds. Substituting this inequality into (B.20), we obtain

$$J_m^a(s^0, \pi_1^2) - J_m^a(s^0, \pi_1^3) \leq 0. \quad (\text{B.21})$$

Based on the characteristics of Π^2 and Π^3 , we observe that the state constraints cannot be satisfied following policy set Π_1^2 , whereas they can be met with policy set Π_1^3 . Therefore, we have

$$\begin{cases} J_m^p(s^0, \pi_1^2) < -\lambda \gamma_m^{t_{\max}}, \\ J_m^p(s^0, \pi_1^3) = 0. \end{cases} \quad (\text{B.22})$$

According to (B.22), we obtain

$$J_m^p(s^0, \pi_1^2) - J_m^p(s^0, \pi_1^3) < -\gamma_m^{t_{\max}} \lambda. \quad (\text{B.23})$$

Based upon (B.8), we have

$$J_m^g(s^0, \pi_1^2) - J_m^g(s^0, \pi_1^3) < \alpha \gamma_m^{t_{\max}} (1 - \gamma_m) < \alpha \gamma_m^{t_{\max}}. \quad (\text{B.24})$$

Below, we calculate $J(s^0, \pi_1^2) - J(s^0, \pi_1^3)$. Referring to (B.4), we have

$$\begin{aligned} J(s^0, \pi_1^2) - J(s^0, \pi_1^3) &= J_m^a(s^0, \pi_1^2) - J_m^a(s^0, \pi_1^3) \\ &\quad + J_m^g(s^0, \pi_1^2) - J_m^g(s^0, \pi_1^3) \\ &\quad + J_m^p(s^0, \pi_1^2) - J_m^p(s^0, \pi_1^3). \end{aligned} \quad (\text{B.25})$$

Incorporating (B.21), (B.23) and (B.24) into (B.25), we obtain

$$J(s^0, \pi_1^2) - J(s^0, \pi_1^3) < \gamma_m^{t_{\max}} (\alpha - \lambda). \quad (\text{B.26})$$

Given that the inequality $\lambda > \alpha \gamma_m^{t_c - t_{\max}}$ in (15) holds, we can substitute it into (B.26) to obtain

$$\begin{aligned} J(s^0, \pi_1^2) - J(s^0, \pi_1^3) &< \gamma_m^{t_{\max}} (\alpha - \alpha \gamma_m^{t_c - t_{\max}}) \\ &= \gamma_m^{t_{\max}} \alpha (1 - \gamma_m^{t_c - t_{\max}}). \end{aligned} \quad (\text{B.27})$$

In that $t_c - t_{\max} \leq 0$ and $0 < \gamma_m < 1$, we have $\gamma_m^{t_c - t_{\max}} \geq 1$. Thus, it can be concluded that

$$J(s^0, \pi_1^2) - J(s^0, \pi_1^3) < 0. \quad (\text{B.28})$$

Hence, we can assert that $J(s^0, \pi_1^3) > J(s^0, \pi_1^2)$, for all $\pi_1^3 \in \Pi^3$ and $\pi_1^2 \in \Pi^2$ with $T_{\pi_1^2} \geq T_{\pi_1^3}$.

Step 8. Prove that $J(s^0, \pi_2^3) > J(s^0, \pi_2^2)$, for all $\pi_2^3 \in$

Π^3 and $\pi_2^2 \in \Pi^2$ with $T_{\pi_2^2} < T_{\pi_2^3}$. For any $\pi_2^2 \in \Pi^2$ and any $\pi_2^3 \in \Pi^3$ with $T_{\pi_2^2} < T_{\pi_2^3}$, the derivation of (B.23) and (B.24) remains valid for policies Π_2^2 and Π_2^3 . Thus, we have

$$\begin{cases} J_m^p(s^0, \pi_2^2) - J_m^p(s^0, \pi_2^3) < -\gamma_m^{t_{\max}} \lambda, \\ J_m^g(s^0, \pi_2^2) - J_m^g(s^0, \pi_2^3) < \gamma_m^{t_{\max}} \alpha. \end{cases} \quad (\text{B.29})$$

Next, let's analyze the magnitude of $J_m^a(s^0, \pi_2^2) - J_m^a(s^0, \pi_2^3)$. Firstly, let's examine the magnitude of $J_m^a(s^0, \pi_2^2)$. According to the definition of t_c in (14), we have $T_{\pi_2^2} \geq t_c$. Hence, we obtain

$$J_m^a(s^0, \pi_2^2) = \gamma_m^{T_{\pi_2^2}} \alpha \leq \gamma_m^{t_c} \alpha. \quad (\text{B.30})$$

Let's assess the magnitude of $J_m^a(s^0, \pi_2^3)$. Based on the definition of the terminal step T_f , we have $T_{\pi_2^3} \leq t_{\max}$. Therefore, we can infer that

$$J_m^a(s^0, \pi_2^3) = \gamma_m^{T_{\pi_2^3}} \alpha \geq \gamma_m^{t_{\max}} \alpha. \quad (\text{B.31})$$

Referring to (B.30) and (B.31), we have

$$J_m^a(s^0, \pi_2^2) - J_m^a(s^0, \pi_2^3) \leq \gamma_m^{t_c} \alpha - \gamma_m^{t_{\max}} \alpha. \quad (\text{B.32})$$

According to (B.4), we have

$$\begin{aligned} J(s^0, \pi_2^2) - J(s^0, \pi_2^3) &= J_m^a(s^0, \pi_2^2) - J_m^a(s^0, \pi_2^3) \\ &\quad + J_m^g(s^0, \pi_2^2) - J_m^g(s^0, \pi_2^3) \\ &\quad + J_m^p(s^0, \pi_2^2) - J_m^p(s^0, \pi_2^3). \end{aligned} \quad (\text{B.33})$$

Substituting (B.29) and (B.32) into (B.33), it holds that

$$J(s^0, \pi_2^2) - J(s^0, \pi_2^3) < -\gamma_m^{t_{\max}} \lambda + \gamma_m^{t_c} \alpha \quad (\text{B.34})$$

Substituting the inequality $\lambda > \alpha \gamma_m^{t_c - t_{\max}}$ in (15) into (B.34), we obtain

$$J(s^0, \pi_2^2) - J(s^0, \pi_2^3) < 0 \quad (\text{B.35})$$

Combining equations (B.28) and (B.35), we can conclude that $J(s^0, \pi^3) > J(s^0, \pi^2)$, for all $\pi^3 \in \Pi^3$ and $\pi^2 \in \Pi^2$.

Thus, it can be concluded that for all $\pi^3 \in \Pi^3$, and for all $\pi^{0,1,2} \in \Pi^0 \cup \Pi^1 \cup \Pi^2$, it holds that $J(s^0, \pi^3) > J(s^0, \pi^{0,1,2})$. Next, we will proceed to prove that for all $\pi^3 \in \Pi^3$ and $\bar{\pi}^3 \in \Pi^3$, if $T_{\pi^3} < T_{\bar{\pi}^3}$ then $J(s^0, \pi^3) > J(s^0, \bar{\pi}^3)$.

Step 9. Prove that $J(s^0, \pi^3) > J(s^0, \bar{\pi}^3)$, for all $\pi^3 \in \Pi^3$ and $\bar{\pi}^3 \in \Pi^3$ with terminal time $T_{\bar{\pi}^3} > T_{\pi^3}$. We analyze the components of $J(s^0, \pi^3)$ and $J(s^0, \bar{\pi}^3)$ sequentially. Since the agent takes time T_{π^3} to reach the terminal state following policy $\pi^3 \in \Pi_3$, and time $T_{\bar{\pi}^3}$

following policy $\bar{\pi}^3 \in \Pi^3$, we have

$$\begin{cases} J_m^a(s^0, \pi^3) = \alpha \gamma_m^{T_{\pi^3}}, \\ J_m^a(s^0, \bar{\pi}^3) = \alpha \gamma_m^{T_{\bar{\pi}^3}}. \end{cases} \quad (\text{B.36})$$

Considering the properties of policy set Π_3 , the state constraints can be satisfied following policies π^3 and $\bar{\pi}^3$. Therefore, we have

$$\begin{cases} J_m^p(s^0, \pi^3) = 0, \\ J_m^p(s^0, \bar{\pi}^3) = 0. \end{cases} \quad (\text{B.37})$$

According to (B.8), we have

$$J_m^g(s^0, \pi^3) - J_m^g(s^0, \bar{\pi}^3) > -\alpha \gamma_m^{t_{\max}} (1 - \gamma_m) \quad (\text{B.38})$$

Based on (B.4), we have

$$\begin{aligned} J(s^0, \pi^3) - J(s^0, \bar{\pi}^3) &= J_m^a(s^0, \pi^3) - J_m^a(s^0, \bar{\pi}^3) \\ &\quad + J_m^g(s^0, \pi^3) - J_m^g(s^0, \bar{\pi}^3) \\ &\quad + J_m^p(s^0, \pi^3) - J_m^p(s^0, \bar{\pi}^3) \end{aligned} \quad (\text{B.39})$$

Substituting equation (B.36), (B.37) and (B.38) into (B.39), we obtain

$$J(s^0, \pi^3) - J(s^0, \bar{\pi}^3) > \alpha (\gamma_m^{T_{\pi^3}} - \gamma_m^{T_{\bar{\pi}^3}}) - \alpha \gamma_m^{t_{\max}} (1 - \gamma_m) \quad (\text{B.40})$$

Given that $T_{\pi^3} < T_{\bar{\pi}^3}$, we can confirm that $T_{\bar{\pi}^3} - T_{\pi^3} \geq 1$. Substituting this inequality into (B.39), we obtain

$$\begin{aligned} &J(s^0, \pi^3) - J(s^0, \bar{\pi}^3) \\ &> \alpha \gamma_m^{T_{\pi^3}} (1 - \gamma_m^{T_{\bar{\pi}^3} - T_{\pi^3}}) - \alpha \gamma_m^{t_{\max}} (1 - \gamma_m) \\ &\geq \alpha \gamma_m^{t_{\max}} (1 - \gamma_m) - \alpha \gamma_m^{t_{\max}} (1 - \gamma_m) \\ &= 0 \end{aligned} \quad (\text{B.41})$$

Thus, we can conclude that for all $\pi^3 \in \Pi^3$ and $\bar{\pi}^3 \in \Pi^3$, if $T_{\pi^3} < T_{\bar{\pi}^3}$ then $J(s^0, \pi^3) > J(s^0, \bar{\pi}^3)$. In conclusion, it can be summarized that among non-constraints-violating policies $\pi^3 \in \Pi^3$, the policy $\pi^{3*} \in \Pi^3$ with the minimal terminal time has the maximum return. Thus, the optimal policy obtained based on (13) satisfies the *minimum-time problem*.

C Proof of Corollary 1

Corollary 1 addresses the *minimum-time problem* without state constraints, which is a special case of the *minimum-time problem* where the feasible state set $C = \mathbb{R}^{np}$ (2f). This connection allows us to apply properties from Theorem 2 for the *minimum-time problem* to Corollary 1 for the unconstrained case.

We first categorize joint policies into two main sets, $\Pi^i, i = 4, 5$, as shown in Table C.1. We then establish the relationship between policy sets Π^4 and Π^1 , and Π^5 and Π^3 , where policy sets Π^3 and Π^1 are the ones consid-

ered in Theorem 2 of Table A.1. Given the feasible state set $C = \mathbb{R}^{np}$ in this corollary, the state constraint (2f) is always satisfied under $\Pi^i, i = 4, 5$. According to the definition of policy set $\Pi^i, i = 1, 3, 4, 5$ in Tables C.1 and A.1, we find that Π^4 and Π^1 , and Π^5 and Π^3 , are consistent in satisfying state and terminal constraints. The only difference between the POMDPs in Corollary 1 and Theorem 2 is the penalty weight λ as shown in (16) and (15), and because the state constraint is satisfied under $\Pi^i, i = 1, 3, 4, 5$, the differing λ values do not impact the return under these policy sets. Thus, the return ranges of Π^1 and Π^4 , which both satisfy the terminal constraint, are consistent, as are those of Π^3 and Π^5 , which do not.

Table C.1

Policy classification

	Satisfy terminal constraint
Π^4	×
Π^5	✓

Next, building on Theorem 2, we demonstrate the relationship between the returns of policies in Π^4 and Π^5 . From **Step 5** of Theorem 2, we have $J(s^0, \pi^3) > J(s^0, \pi^1)$ for all $\pi^3 \in \Pi^3$ and $\pi^1 \in \Pi^1$. Given the consistency between Π^1 and Π^4 , and Π^3 and Π^5 , it follows that $J(s^0, \pi^5) > J(s^0, \pi^4)$ for all $\pi^5 \in \Pi^5$ and $\pi^4 \in \Pi^4$. According to **Step 9** of Theorem 2, $J(s^0, \pi^3) > J(s^0, \bar{\pi}^3)$ for all $\pi^3 \in \Pi^3$ and $\bar{\pi}^3 \in \Pi^3$ where $T_{\bar{\pi}^3} > T_{\pi^3}$. By the consistency of Π^3 and Π^5 , we have $J(s^0, \pi^5) > J(s^0, \bar{\pi}^5)$ for all $\pi^5 \in \Pi^5$ and $\bar{\pi}^5 \in \Pi^5$ with $T_{\bar{\pi}^5} > T_{\pi^5}$. In conclusion, among policies $\pi^5 \in \Pi^5$ that do not violate terminal constraints, the policy $\pi^{5*} \in \Pi^5$ with the minimal terminal time maximizes the return. Thus, the optimal policy derived from (13) meets the *minimum-time problem without state constraints*.